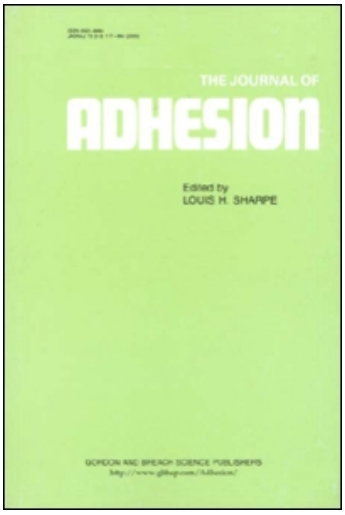

The Journal of Adhesion
Publication details, including instructions for authors and subscription information:
http://www.informaworld.com/smpp/title~content=t713453635

Purification of DOPA-Containing Foot Proteins from Green Mussel, *Perna viridis*, and Adhesive Properties of Synthetic Model Copolypeptides

Kousaku Ohkawa[a]; Tadahiro Nagai[a]; Ayako Nishida[a]; Hiroyuki Yamomoto[a]
[a] Institute of High Polymer Research, Faculty of Textile Science and Technology, Shinshu University, Japan

Online publication date: 12 November 2009

To cite this Article Ohkawa, Kousaku , Nagai, Tadahiro , Nishida, Ayako and Yamomoto, Hiroyuki(2009) 'Purification of DOPA-Containing Foot Proteins from Green Mussel, *Perna viridis*, and Adhesive Properties of Synthetic Model Copolypeptides', The Journal of Adhesion, 85: 11, 770 — 791
To link to this Article: DOI: 10.1080/00218460903291353
URL: http://dx.doi.org/10.1080/00218460903291353

The Journal of Adhesion, 85:770–791, 2009

ISSN: 0021-8464 print/1545-5823 online
DOI: 10.1080/00218460903291353

Taylor & Francis
Taylor & Francis Group

Purification of DOPA-Containing Foot Proteins from Green Mussel, *Perna viridis,* and Adhesive Properties of Synthetic Model Copolypeptides

Kousaku Ohkawa, Tadahiro Nagai, Ayako Nishida, and Hiroyuki Yamomoto
Institute of High Polymer Research, Faculty of Textile Science and Technology, Shinshu University, Japan

The thread-like adhesive tissue of the green mussel, Perna viridis, *is referred to as the byssus. The phenol gland-derived proteins are involved in the underwater adhesion of the byssus. The objectives of the present study are identification and characterization of the phenol gland-derived proteins in the foot of* P. viridis*.* P. viridis *foot contains at least eight kinds of potential precursor proteins, designated as* P. viridis *foot proteins (Pvfp)-a to -h. Among the precursors, Pvfp-g and Pvfp-h are found at relatively high levels in the phenol gland. These proteins are considered to be essential components in the adhesive plaque, which mediates adhesion of the thread to the substrate surface. Both Pvfp-g and Pvfp-h are enriched in* L*-*β*-3,4-dihydroxyphenyl-*α*-alanine (DOPA), tyrosine (Tyr) and cysteine (Cys), as well as glycine (Gly) and lysine (Lys). According to the amino acid compositions in Pvfp-g and Pvfp-h, two copolypeptides containing four amino acids, Cys, Tyr, Gly, and Lys, were synthesized as the biomimetic model materials. The copolypeptides were subjected to the tyrosinase-catalyzed oxidation, followed by tensile shear strength test. The results suggest that DOPA and Cys in Pvfp-g and Pvfp-h cooperatively contribute to rapid protein cross-linking, enhancing the cohesive strength of the matrix of the adhesive plaque.*

Keywords: Adhesive protein; Characterization; Enzymatic oxidation; Green mussel; Synthetic copolypeptide; Tyrosinase

Received 7 November 2008; in final form 22 April 2009.

One of a Collection of papers honoring J. Herbert Waite, the recipient in February 2009 of *The Adhesion Society Award for Excellence in Adhesion Science, Sponsored by 3M*.

Address correspondence to Kousaku Ohkawa, Institute of High Polymer Research, Shinshu University, Tokida 3-15-1, Ueda 386-8567, Nagano Prefecture, Japan. E-mail: kohkawa@giptc.shinshu-u.ac.jp

1. INTRODUCTION

Adhesion capabilities of living organisms have attracted researchers for a prolonged period. In the last two decades, understanding of chemistry involved in the biogenic adhesive capabilities has undergone remarkable progress, encompassing a wide variety of organisms, including bacteria [1,2], polycheates [3,4], mollusks [5–7], crustaceans [8–10], insects [11,12], and spiders [13,14]. These adhesives are commonly non-cellular materials, which are secreted outside of the animal bodies and then cure or harden *via* polymer chemical and/or enzymatic processes. In parallel with the progress in biology and biochemistry on biological adhesives, polymer chemical studies have significantly contributed to development of synthetic bio-adhesives and related compounds and also to reveal adhesive mechanisms using synthetic models, subsequently exploring novel bio-inspired material chemistry [15].

One of the major components of biogenic adhesives is protein, of which essence in the curing processes are classified into two groups: one typically involves non-covalent protein–protein aggregation or cohesion, leading to insolubilization of the secreted adhesives, for instance, as seen in barnacle cement [8] and the caddis fly larva net [11]. The other one depends on the enzymatic actions to ensure the surface chemical reaction between the adhesive proteins and the substrates [16], followed by protein–protein cross-linking [17] to turn the soluble precursor substances into insoluble and often chemically resistant adhesive materials [18]. One family of marine mussels, the Mytilidae, has been investigated for biochemical and polymer chemical aspects associated with the biogenesis of their underwater adhesive organs, referred to as "byssus" [19]. Byssus can be classified in the latter group of the biogenic adhesives, utilizing the surface active proteins and the oxidative enzyme in their hardening mechanisms.

Single byssus is a thread-like, non-cellular, and extra-organismic adhesive [20], of which the distal end of the thread adheres onto the substrate, while the proximal end is bundled into a thread that is connected to the byssal retractor muscle. As the mussels attach on a given underwater substrate, routinely 30–40 threads are formed. The biogenesis of individual byssus threads occurs in the ventral groove along the longer axis of the mussel foot, and the distal extreme of the groove ends with a specific tissue, known as the phenol gland, where the precursor proteins of the byssus threads adhesives are stored. Hence, the distal end of the single byssus thread adheres onto the substrate with a hardened pad-like structure, *i.e.*, an adhesive plaque.

The adhesion mechanism of *Mytilid* mussels has been thoroughly investigated on a marine blue mussel, *Mytilus edulis*, in which at least five adhesive precursor proteins plus three collagen-like proteins are involved in the byssus thread formation. Waite *et al.* have confirmed that a characteristic amount of a unusual amino acid, L-β-3,4-dihydroxyphenyl-α-alanine (L-DOPA), is definitely contained in all precursor proteins of the byssus adhesives in the settlement of *M. edulis* [21]. These proteins were designated as *M. edulis* foot proteins, (Mefps)-1 to -5. Mefp-1 to Mefp-5 were shown to play different roles in byssal adhesion and, in particular, Mefp-3 and Mefp-5 were shown to be surface active components (primer) and specifically localized to the plaque. Also, in the other related marine mussel adhesives, DOPA contributes to both the surface-coupling and the protein cross-linking reactions [5].

In a previous study, we established that in another *Mytilid* species, the green mussel *Perna viridis*, eight kinds of the DOPA-containing precursor proteins were present in the foot [22]. The identified proteins were designated as *P. viridis* foot proteins (Pvfps). Since the Pvfp protein precursors were found to be more diverse than those found in *M. edulis*, the roles of the Pvfps in byssus adhesion can be considered as the corresponding counterparts among the other foot proteins, which have been found so far in *Mytilid* mussels. Hence, a model study on the roles of the precursors in the *P. viridis* adhesive plaque is required for deeper insight into the shared and unique features of the adhesive mechanisms among *Mytilid* mussels.

The objectives of the present study are (i) identification of phenol gland-derived protein(s) of *P. viridis* foot as putative active ingredients of underwater adhesion, (ii) synthesis of the model copolypeptides having the pre-determined amino acid composition, which is characteristic for the native phenol gland-specific protein(s), and (iii) the enzyme-mediated oxidation of the synthetic copolypeptides, followed by adhesive tests in order to clarify the roles of the phenol coupling involved in underwater adhesion of the *P. viridis* byssus.

2. MATERIALS AND METHODS

2.1. Materials

The green mussels, *P. viridis*, were collected from the rocky shore in Kanagawa Prefecture, Japan. The mussel foot was dissected at the proximal root, then rinsed briefly in a phosphate buffer (pH 7.2) containing 10 mM KCN, and immediately frozen on dry ice. The dissected feet were stored at -80°C until use.

2.2. Preparation of *Perna viridis* Foot Extract

The frozen mussel feet were thawed on ice and the brownish pigment on the foot surface was carefully removed by wiping with paper. The muscle of the foot tip and sides were removed using a sharp knife, and the light yellowish tissue around the ventral groove and the phenol gland (byssus forming tissue complex, BFTC) was recovered, briefly rinsed in 5.0% acetic acid (AcOH), then immersed in an extraction solution containing 5.0% AcOH, 0.5% methanol, 1.0 mM KCN, 30 μM pepstatin A, and 20 μM leupeptin. Approximately 60 BFTCs were homogenized in 50 mL of extraction solution, using a glass homogenizer with a poly(tetrafluoroethylene) pestle. After five strokes, the homogenate was recovered, and then centrifuged at 14,500 rpm for 30 min at 4°C. The supernatant was transferred to a beaker in an ice-cooled bath, and, with stirring, 60% perchloric acid (PCA) was added to adjust the final PCA concentration of 1.0%. The precipitate was removed by centrifugation at 14,500 rpm for 20 min at 4°C. The supernatant was transferred into a beaker in an ice-ethanol bath (*ca.* −15°C), and with stirring, concentrated sulfuric acid was added to the final concentration of 0.3 M, followed by drop-wise addition of pre-chilled acetone (−80°C) to the final acetone concentration of 33%. White aggregates were soon separated from the mixture and the mixture was stirred for 30 min. The aggregates were recovered by centrifugation at 14,500 rpm for 15 min at 4°C. The recovered white aggregate was dissolved again in 5.0% AcOH containing 2.0 M urea. This solution was stored at −80°C, and just before further use, it was thawed and centrifuged to remove the insoluble materials.

2.3. Assay of *Perna viridis* Foot Proteins (Pvpfs)

The protein composition was assayed by means of acid-urea poly(acryl amide) gel electrophoresis (AU-PAGE) [22]. The development of the protein band was performed by two staining methods: coommasie brilliant blue R250 (CBBR) for total protein and nitroblue tetrazolium chloride (NBT) for the DOPA-containing proteins. Both CBBR and NBT were obtained from Wako Pure Chemical Industry, Osaka, Japan.

2.4. Localization of Pvfps in Foot Tissue

The BFTC were divided into eight pieces across the distal-to-proximal axis, in which the phenol gland near the distal tip was included in the second piece. Thus, the distal tip (the first piece) mostly contains the foot

muscle. The Pvfps in each of the eight pieces were extracted by the same procedure described above. The protein compositions in the eight extracts were assayed by means of AU-PAGE. The resolved protein bands on the AU-PAGE gel were stained with CBBR and NBT, and the developed bands were optically scanned for the densitometry to compare the relative contents of the foot proteins in each of the eight pieces.

2.5. Purification of Pvfps

The *P. viridis* foot extract (2.0 mL) was first passed through a gel filtration column, Sephacryl S-300 HiPrep16/30 (Amersham-Pharmacia, Tokyo, Japan), which was equilibrated with 5.0% AcOH containing 2.0 M urea at the flow rate of 1.0 mL/min. The fractions eluted from 54–65 min were recovered and pooled. Next, the pooled fractions were dialyzed against 5.0% AcOH at 4°C and lyophilized. The residue was re-dissolved in 450 μL of 5.0% AcOH then loaded onto a gel permeation chromatography column, Shodex KW803 (8 × 300 mm, Showa Denko, Co. Ltd., Tokyo, Japan), which was equilibrated with 5.0% AcOH containing 0.1% trifluoroacetic aicd at the flow rate of 0.5 mL/min. The fractions eluted from 19.5 to 20.5 min were pooled as pure Pvfp-g and from 21.0 to 22.0 min were as pure Pvfp-h. Two preparations were lyophilized and stored at −20°C until use.

2.6. Amino Acid Composition Analysis

The purified preparations of Pvfp-g and Pvfp-h (*ca.* 0.1 mg each) were placed in ampoule bottles and dissolved in 10 μL of the Milli-Q™ water. A 50% propionic acid solution containing 6 N HCl and 10% phenol (200 μL) was added to the sample solutions, then the ampoules were sealed *in vacuo* using an oxygen torch. The sealed samples were heated at 110°C for 24 hr. The hydrolysates were dried up and then re-dissolved in a citrate buffer (pH 3.2, Wako Pure Chemical Industry, Osaka, Japan). The sample solutions were loaded onto an automated amino acid composition analysis system (LCVp-10AT System, Shimadzu, Kyoto, Japan). The analysis was performed according to our previous report [22].

2.7. Synthesis of Pvfp-Derived Copolypeptides

All chemicals used in the synthesis of the copolypeptides were purchased as reagent grades. The solvents in the synthesis of NCAs were purified by distillation from sodium (for *n*-hexane, 1,4-dioxane, and diethyl ether) and from P_2O_5 (for ethyl acetate). Benzyloxycarbonyl

(Z) group was chosen for the side-chain protection of the amino acids. *N*-carboxyanhydrides (NCAs) of Cys(Z), Tyr(Z), Gly, Lys(Z) were first prepared and then copolymerized in the presence of a base as catalyst for polycondensation [23,24]. The feed ratios of four NCAs were designed on the basis of the amino acid compositions found in native Pvfp-g and Pvfp-h. After the polycondensation, the side-chain protecting groups, Z, were removed by acidic fission. The resulting polypeptides were designated as the copolypeptide-g and copolypeptide-h, respectively, for the Pvfp-g-derived and the Pvfp-h-derived amino acid compositions. Methods for the preparation of the monomer NCAs and three copolypeptides are presented in the following sections.

2.7.1. N^{α},S-Di-Benzyloxycarbonyl-L-Cysteine (Z-Cys(Z)) (1)

L-Cys monohydrochloride monohydrate (10.0 g, 57 mmol) was dissolved in 2 M NaOH (83 mL, 166 mmol). Under vigorous shaking, Z-C1 (23.4 g, 137 mmol) and 2 M NaOH (31 mL, 62 mmol) were alternately added in portions. After 30 min, diethyl ether was added, and in a separating vessel, unreacted Z-Cl was removed. The aqueous layer was acidified with 3 M HCl to pH 3.0, and precipitated oil was extracted with ethyl acetate. The organic layer was recovered and dried on anhydrous disodium sulfate. After evaporation, the crude product was crystallized from *n*-hexane, then re-crystallized from tetrachloromethane–*n*-hexane. The yield of Z-Cys(Z) was 16.6 g (75%).

2.7.2. Cys(Z) NCA (2)

Z-Cys(Z) (4.3 g, 11 mmol) was dissolved in 30 mL of ethyl acetate. On cooling with an ice bath, PCl_5 (2.5 g, 12 mmol) was added. After dissolution of PCl_5, the reaction mixture was evaporated under reduced pressure. Dry *n*-hexane was added to the residue and the crude product was crystallized, followed by filtration for recovery. The crude product was re-crystallized twice with dry ethyl acetate–*n*-hexane. The yield of Cys(Z) NCA was 2.6 g (84%).

2.7.3. N^{α},O-Di-Benzyloxycarbonyl-L-Tyrosine (Z-Tyr(Z)) (3)

L-Tyr (10.0 g, 55 mmol) was dissolved in 2 M NaOH (30 mL, 60 mmol). The reaction was performed by a similar procedure as described for Z-Cys(Z), using Z-Cl (20.6 g, 121 mmol) and 2 M NaOH (60 mL, 120 mmol). The crude product was re-crystallized from ethyl acetate–*n*-hexane. The yield of Z-Tyr(Z) was 21.7 g (88%).

2.7.4. Tyr(Z) NCA (4)

Z-Tyr(Z) (5.8 g, 13 mmol) was dissolved in 60 mL of dry benzene. The trace water in the material was removed as the benzene azeotrope

(*ca.* 10 mL). After the distillation, PCl_5 (2.9 g, 14 mmol) was added to the Z-Tyr(Z)-benzene solution at room temperature. The reaction mixture was stirred for 30 min and evaporated under reduced pressure. The residue was crystallized with dry *n*-hexane. The crude product was re-crystallized twice from dry benzene–*n*-hexane. The yield of Tyr(Z) NCA was 3.6 g (82%).

2.7.5. N^{α}-Benzyloxycarbonyl-Glycine (Z-Gly) (5)

Gly (7.5 g, 100 mmol) was dissolved in 4 M NaOH (25 mL, 100 mmol). The reaction was performed by a similar procedure as described for Z-Cys(Z), using Z-Cl (18.8 g, 110 mmol) and 4 M NaOH (30 mL, 120 mmol). The crude product was re-crystallized from tetrachloromethane–*n*-hexane. The yield of Z-Gly was 17.3 g (83%).

2.7.6. Gly NCA (6)

Z-Gly (2.3 g, 11 mmol) was dissolved in 30 mL of dry ethyl acetate. On cooling, PCl_5 (2.3 g, 11 mmol) was added and stirred for 30 min. The reaction mixture was evaporated under reduced pressure, and dry *n*-hexane was added to the residue for crystallization of the crude product. The crude product was re-crystallized twice from dry 1,4-dioxane–*n*-hexane. The yield of Gly NCA was 0.94 g (85%).

2.7.7. N^{α},N^{ε}-Di-Benzyloxycarbonyl-L-Lysine (Z-Lys(Z)) (7)

L-Lys monohydrochloride (10.0 g, 55 mmol) was dissolved in 2 M NaOH (55 mL, 110 mmol). The reaction was performed by a similar procedure as described for Z-Cys(Z), using Z-Cl (20.6 g, 121 mmol) and 4 N NaOH (30 mL, 120 mmol). The crude product was re-crystallized from ethyl acetate-*n*–hexane. The yield of Z-Lys(Z) was 17.6 g (77%).

2.7.8. Lys(Z) NCA (8)

Z-Lys(Z) (4.6 g, 11 mmol) was dissolved in ethyl acetate (15 mL). On cooling, PCl_5 (2.3 g, 11 mmol) was added and stirred for 20 min. The reaction mixture was evaporated under reduced pressure, and dry *n*-hexane was added to the residue for crystallization of the crude product. The crude product was re-crystallized twice from dry ethyl acetate-*n*–hexane. The yield of Lys(Z) NCA was 2.7 g (79%).

2.7.9. Polycondensation of NCAs

The feed molar ratio of four kinds of amino acid NCAs for the protected copolypeptide-g (Scheme 1, compound 9) was Cys(Z) NCA:Tyr(Z) NCA:Gly NCA:Lys(Z) NCA = 27:38:22:13 and that for the protected copolypeptide-h (10) was Cys(Z) NCA:Tyr(Z) NCA:Gly NCA:Lys(Z) NCA = 33:29:21:17. As a reference sample for polycondensation,

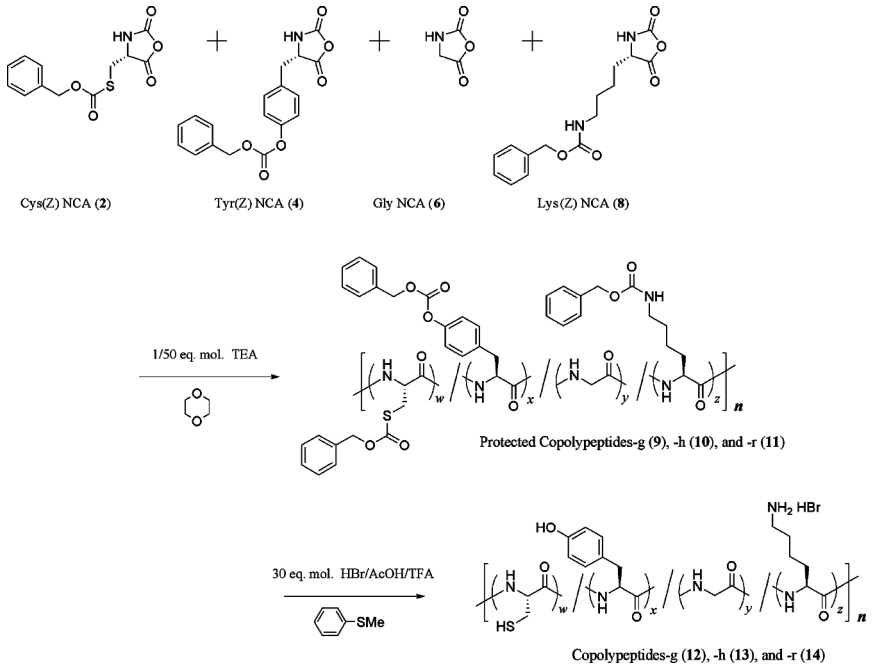

SCHEME 1 Synthesis of the Pvfp-g- and Pvfp-h-derived copolypeptides. The feed ratios of NCAs are represented in Table 2, together with the observed ratios of the amino acids (*w, x, y*, and *z*) after completion of the synthesis.

an equi-molar mixture of four NCAs, Cys(Z) NCA:Tyr(Z) NCA:Gly NCA:Lys(Z) NCA = 25:25:25:25, was also prepared as the protected copolypeptide-r (11). The feed solutions of copolypeptide-g, copolypeptide-h, and copolypeptide-r were prepared by dissolving the NCAs in dry l,4-dioxane at the pre-determined ratios as described above. Triethylamine (TEA) was added to three feed solutions at molar ratios of TEA:total NCAs = 1:50. The initiation of polycondensation was confirmed by generation of CO_2 bubbles in the reaction mixture. The reaction continued for 72 h at room temperature, then terminated upon heating at 80°C for 2 h. The reaction mixtures were evaporated under reduced pressure, then the copolypeptides were precipitated with water. After, the precipitates were repeatedly washed with water, then dried *in vacuo*. The yields of the protected copolypeptide-g, copolypeptide-h, and copolypeptide-r were 77%, 65%, and 77%, respectively.

Degrees of polymerization (*Dp*s) were estimated for the protected copolypeptides-g (9), -h (10), and -r (11) on the basis of the viscosity

average molecular weight measurements. The *Dp*s are calculated with the observed intrinsic viscosity $[\eta]$ of copolypeptides in dichroloacetic acid solution at 25.0°C.

i. $[\eta] = 3.20 \times 10^{-4}\ M_V^{066}$ for poly[Tyr(Z)] [25]
ii. $\log Dp = 1.47 \times \log[\eta] + 2.99$ for poly[Lys(Z)] [26]

The *Dp*s obtained for the protected copolypeptides were used for the calculation of molecular weights of the deprotected copolypeptides (compounds 12–14) as described in the following sections.

2.7.10. Removal of Side-Chain Protecting Groups

The protected copolypeptides-g (9), -h (10), and -r (11) were separately dissolved in trifluoroacetic acid, and thioanisole (1.0 equivalent molar toward Z groups) was added to the solutions. With stirring, 25% HBr in AcOH solution (10 equivalent molar towards Z groups) was added to each solutions. The reaction was performed for 8 h. A small portion of the reaction mixture was sampled for monitoring the removal of Z groups from copolypeptide, and complete deprotection was confirmed by disappearance of the UV-absorption band at 254 nm of Z groups. The reaction mixtures were evaporated under reduced pressure, and diethylether was poured over the residues to precipitate the deprotected copolypeptides. The crude products were washed repeatedly with diethyl ether, then re-precipitated from water–ethanol–diethyl ether. The yields of the deprotected copolypeptide-g (12), copolypeptide-h (13), and copolypeptide-r (14) were 86%, 88%, and 90%, respectively.

2.7.11. Characterization of Synthetic Copolypeptides

The amino acid composition analyses of the deprotected copolypeptides-g, -h, and -r were carried out by the same method as described in Section 2.6. On the basis of the observed amino acid compositions, the molecular weights of the deprotected copolypeptides-g, -h, and -r were calculated with the *Dp*s obtained for the corresponding protected copolypeptides. Fourier transform infrared spectra of the deprotected copolypeptides-h (12), -g (13), and -r (14) were recorded using a Horiba FT720 apparatus, Kyoto, Japan. The samples were prepared as KBr pellets.

2.8. Enzyme-Mediated Oxidation of Synthetic Copolypeptides

The copolypeptides-g (12), -h (13), and -r (14) were dissolved in distilled water (12 mM amino acid residues), and the pH values were

adjusted at 6.5 by addition of 4 M NaOH. The copolypeptide solution (530 μL), 1.0 M ascorbic acid (160 μL, pH 6.5), and 10 mg/mL tyrosinase solution (E.C. 232-653-4; Sigma-Aldrich, Tokyo, Japan, lot No. 124K7038, 3320 units/mg solid) (51 μL) were mixed and then diluted with distilled water to give the final volume of 1.6 mL. The final concentrations of copolypeptide, tyrosinase, and ascorbic acid in the reaction mixture were 4.0 mM, 0.32 mg/mL, and 100 mM, respectively. At the pre-determined reaction times of 0.5, 1, 2, 4, 12, and 20 h, a portion of the reaction mixture (50 μL) was sampled and then immediately the reaction was terminated by addition of 5.0 M methanesulfonic acid (200 μL). The sampled solutions were transferred in ampoule bottles and sealed *in vacuo* using an oxygen torch. The sealed ampoules were heated at 115°C for 24 h, followed by neutralization by addition of 3.5 M NaOH (250 μL). The mixtures were further diluted with a citrate buffer (pH 3.2, Wako Pure Chemical Industry, Osaka, Japan) and subjected to amino acid composition analysis in order to determine the contents in molar percentages of Tyr and DOPA.

2.9. Measurement of Tensile Shear Strength

Iron and alumina test pieces were chosen as the substrates for tensile shear strength measurements. The substrates were pre-treated according to Japan Industrial Standard method (JIS K6848-l976, JIS K6859-1976). In brief, the surfaces of the test pieces were polished with a sand paper #240, wiped repeatedly with trichloroethylene, and then dried. The copolypeptides-g (12), -h (13), and -r (14) were dissolved in distilled water at 20 w/v% (pH 6.5, adjusted with 4 M NaOH). The copolypeptide solution (25 μL) was mixed with tyrosinase solution (1.0 w/v%, 25 μL) and then immediately spread onto the pretreated substrate surface. A control experiment was conducted in the absence of tyrosinase. Two substrate pieces were attached to one another with an overlap area of *ca.* 2.4 cm^2, fixed with a clamp, and allowed to stand until dryness under an incubation temperature of 25°C and relative humidity of $50 \pm 5.0\%$.

The specimen was set on a mechanical testing machine (SV-50, Imada, Co., Ltd., Toyohashi, Japan). The shear load was generated at 10 mm/min, and the breaking load values were recorded for at least 8–10 tests to estimate the average strength. The tensile shear strength was represented as the breaking load per attaching area (kgf/cm^2).

3. RESULTS AND DISCUSSION

3.1. Localization of DOPA-Containing Proteins in *Perna viridis* Foot

The precursor proteins of byssus are stored in cells of the ventral groove, which runs along the long axis of the foot. A single byssus fiber is composed of three different parts, namely, adhesive plaque, distal thread, and proximal thread. The precursor proteins of the adhesive plaque are secreted from the phenol gland which is located at the distal end of the ventral groove.

The dissected byssus-forming tissue complex of the mussel foot (BFTC, Fig. 1A) was first divided into eight pieces across distal-to-proximal axis of the mussel foot, in which the second piece contained the phenol gland. The acid soluble proteins extracted from each piece were assayed on AU-PAGE (Fig. 1B), and subsequently the proteins in the gel were stained with CBBR and NBT. The CBBR-staining indicated that the protein composition in the BFTC is completely different from those of the tip and sides of foot muscular tissues (Fig. 1B). Almost all of the BFTC proteins were stained with NBT, indicating that the acid-soluble extract of the BFTC contains certain redox active chromophores (Fig. 1B, lower panel). The NBT-positive chromophores are highly possibly identical to DOPA, on the basis of our previous report [22]. At least eight kinds of NBT-positive protein bands were observed, and the proteins were designated alphabetically, where the protein band having the lowest mobility was denoted as "Pvfp-a," hence the eight NBT-positive bands should be "Pvfp-a" to "Pvfp-h."

In our previous study on the *P. viridis* foot proteins [22], the Pvfp bands were designated as Pvfp-1 to -8. In the present study, the Pvfps are temporarily designated in alphabetical sequence due to the following reasons: (i) one of the purposes in the present study is to determine the putative pairs of the functional counterparts as byssal precursor proteins between *P. viridis* and *M. edulis*; (ii) in the case of *M. edulis*, the *M. edulis* foot proteins (Mefps)-1 to -5 have been already identified with their molecular characteristics and also roles in byssal adhesion; (iii) on the other their hand, at this time, the roles of the Pvfps were mostly unknown; (iv) so that, after characterization of the subjected Pvfps, the corresponding numbers of Mefps could be put on the Pvfps as the counterpart components in *P. viridis* byssal precursor proteins. For example, "Pvfp-a" has been designated as "Pvfp-1," since it has similar consensus amino acid sequences as compared with those of Mefp-1. As for the other Pvfps, their roles still remained to be characterized.

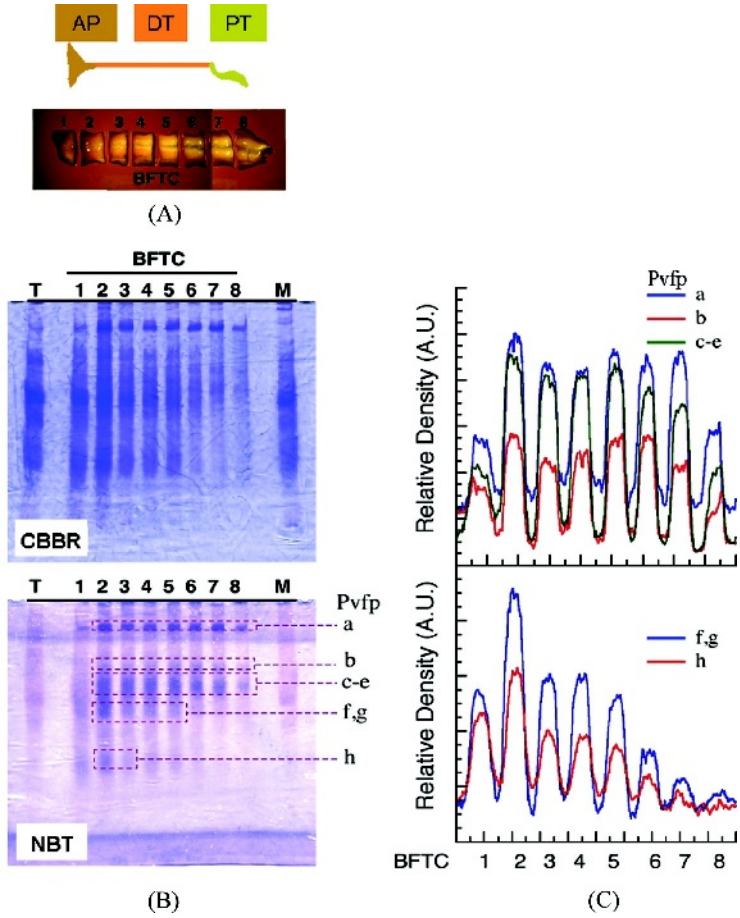

FIGURE 1 Localization of byssus precursor proteins along *Perna viridis* foot. (A) A dissected byssus forming tissue complex (BFTC) which is divided into the eight pieces. The second piece contains the phenol gland, where the precursor proteins of adhesive plaque (AP) were stored. "DT" and "PT" denote distal and proximal threads, respectively. (B) AU-PAGE analysis of the acid extract of the BFTC pieces (lanes 1–8). Lanes "T" and "M" represent the extracts from tip and side muscular tissues of the foot, respectively. After the electrophoresis, gels were stained with CBB for all proteins and NBT for DOPA-containing proteins. The NBT-positive bands were indicated on the right side of the NBT-stained gel (Pvfp-a–Pvfp-h). (C) Densitometries of the NBT-positive bands. Pvfp-g and Pvfp-h were found at the highest density on the second piece (phenol gland) of BFTC.

Figure 1C represents the densitometry of the color intensity for the NBT-positive protein bands. The Pvfp-a is located on near the origin (top of the gel). The scanned areas in densitometry for the protein bands are indicated as rectangular boxes in Fig. 1B (lower panel), and the integrated counts were represented as relative density values on the vertical axis in Fig. 1C. The intensities of protein bands, Pvfp-a to Pvfp-e, were almost constant from second to seventh BFTC pieces; on the other hand, the intensities of the first and eighth piece, were relatively lower than others, since the first and eighth pieces are composed of mostly foot muscles (Fig. 1C, upper panel). This result suggests that the proteins, Pvfp-a to Pvfp-e, are stored in almost equal quantities in all parts of the BFTC. In contrast, the Pvfp-f, -g, and -h were found in their highest amounts at the second piece of the BFTC, where the phenol gland is located (Fig. 1C, lower panel).

The gradually increasing intensities of the Pvfp-f, -g, and -h bands from the proximal (the seventh piece) towards the second piece of the BFTC is also observed. The intensities of the NBT-positive proteins in the first piece sharply decreased due to the higher content of muscular proteins in the distal-most (the first) piece. These results clearly indicated that at least two proteins, Pvfp-g and Pvfp-h, are the phenol gland-specific components and also suggested that Pvfp-g and Pvfp-h are responsible for the formation of the adhesive plaque of *P. viridis* byssus. Therefore, Pvfp-g and Pvfp-h were subjected to purification and further characterization.

3.2. Purification and Characterization of Pvfp-g and Pvfp-h

The acid soluble proteins of *P. viridis* foot were first separated on a gel filtration column. Two major fractions were obtained: the first fraction contains mainly Pvfp-a to Pvfp-f and the second fraction includes Pvfp-g and Pvfp-h, as well as several minor contaminant proteins which were negative toward the NBT-staining. The second fraction was dialyzed against urea-free 5.0% AcOH and lyophilized. The samples were loaded onto a gel permeation column as the final step of purification. Figure 2 represents the elution profile. Two elution peaks of Pvfp-g and Pvfp-h were found at 19.7 and 21.3 min, respectively. The AU-PAGE analysis of the fractions around the elution peaks revealed that both Pvfp-g and Pvfp-h were recovered as electrophoretically pure preparations. The SDS-PAGE analysis of two preparations indicated that both Pvfp-g and Pvfp-h were apparently homogeneous. The estimated molecular weights were 32 and 23 kDa for Pvfp-g and Pvfp-h, respectively (data not shown).

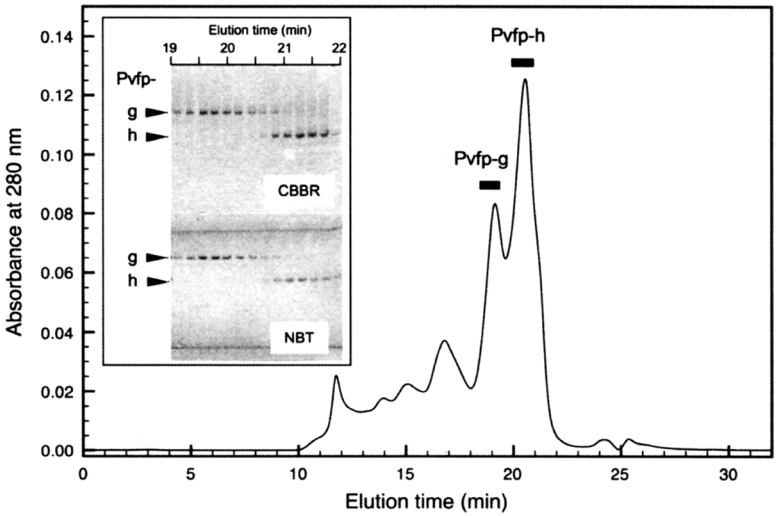

FIGURE 2 Elution profile of gel permeation chromatography on Shodex KW803. The flow rate was 0.5 mL/min. The fractions were collected in 0.25 mL each. Inset indicates AU-PAGE analysis on the protein compositions in the fractions around two elution peaks of Pvfp-g and Pvfp-h. The gels were stained with CBBR for all proteins and with NBT for DOPA-containing proteins. Both Pvfp-g and Pvfp-h were purified as single bands.

The acid hydrolysates of the Pvfp-g and Pvfp-h were analyzed for amino acid composition. The results are summarized in Table 1. Two unusual amino acids, *trans*-4-hydroxy-L-proline (Hyp) and DOPA, can be quantified according to our previous method [22]. As for the chromatographic separations of the amino acids, especially such as Leu and DOPA, which tend to co-elute, we have already optimized the experimental condition for amino acid analysis of the DOPA-containing proteins. The compositions of amino acids are represented as residues per thousand (RPT). The enriched amino acids in Pvfp-g are Cys (148 RPT), DOPA (136 RPT), and Gly (120 RPT). Similar characteristic compositions were obtained for the Pvfp-h, as Cys (186 RPT), Gly (116 RPT), Lys (97 RPT), and DOPA (91 RPT). Since DOPA is an oxidized derivative of Tyr residue, total contents of DOPA plus Tyr could be adjusted to 213 RPT (136 + 77) for the Pvfp-g and 162 RPT (91 + 71) for the Pvfp-g in the whole composition. Hence, Pvfp-g and Pvfp-h are enriched in DOPA and its precursor, *i.e.*, Tyr residues. Also, Cys and Gly residues are common characteristic amino acids in both Pvfp-g and Pvfp-h. Lys is found in the Pvfp-g as 74 RPT, and this value is relatively higher than other amino acids composed of the Pvfp-g.

TABLE 1 Amino Acid Compositions of *Perna viridis* Foot Proteins

	Contents (residue per thousand, RPT)	
Amino acids	Pvfp-g	Pvfp-h
Cys	148	186
DOPA	136	91
Tyr	77	71
(DOPA + Tyr)	(213)	(162)
Gly	120	116
Lys	74	97
Asp + Asn	75	65
Ser	66	68
Leu	83	25
Pro	52	45
Arg	42	47
G1u + Gln	37	25
Thr	16	34
Ala	29	16
Ile	17	15
Cys-Cys	9	19
Val	6	20
Phe	8	18
His	5	18
Hyp	0	16
Met	0	8
Total	1000	1000

On the basis of the amino acid compositions, subsequently, we designed two synthetic model copolypeptides for further experiments.

3.3. Synthesis of Pvfp-g- and Pvfp-h-Derived Copolypeptides

In order to synthesize Pvfp-g- and Pvfp-h-inspired copolypeptides, we chose four enriched amino acids composed of native Pvfp-g and Pvf-h, namely, Cys, Tyr, Gly, and Lys. In the synthetic strategy of the Pvfp-g- and Pvfp-h-derived copolypeptides (Scheme 1, compounds 12, 13), we conducted the preparation of N^{α},*S*-di-Z-Cys (**1**), N^{α},*O*-di-Z-Tyr (3), and N^{α},N^{e}-di-Z-Lys (**7**), followed by the PCl_5-mediated cyclization to yield the amino acid *N*-carboxyanhydrides (2, 4, 8) having the protecting groups Z on their side-chain functionalities. The Gly NCA (6) can be obtained by the same cyclization reaction from N^{α}-Z-Gly (5). The protected NCAs were subjected to a polycondensation reaction in the presence of TEA as the catalyst. The feed monomer ratios are summarized in Table 2. Three kinds of feed nonomer ratios were designed for the Pvfp-g-derived copolypeptide (designated as the copolypeptide-g)

TABLE 2 Synthesis of Model Copolypeptides

	Copolypeptides		
	-g	-h	-r
Protected copolypeptides			
NCAs feed (molar %)[a]			
Cys(Z) NCA	27	33	25
Tyr(Z) NCA	38	29	25
Gly NCA	22	21	25
Lys(Z) NCA	13	17	25
Degree of polymerzation (Dp)[b]	56	56	51
Deprotected copolypeptides			
Amino acids found (molar %)[c]			
Cys	24	31	23
Tyr	40	30	27
Gly	21	20	24
Lys	15	19	26
Calculated M_w[d]	7500	7450	6940

[a]Designed from amino acid compositions in native Pvfp-g and Pvfp-h. "-r" denotes a reference experiment in equi-molar mixture of NCAs.
[b]Estimated by viscosity measurement.
[c]Determined by acid hydrolysis and subsequent amino acid composition analysis.
[d]Calculated from values in b) and c).

as Cys(Z) NCA:Tyr(Z) NCA:Gly NCA:Lys(Z) NCA = 27:38:22:l3 and for the Pvfp-h-derived copolypeptide (copolypeptide-h) = 33:29:21:17. Tyr was introduced to the copolypeptide as the precursor of DOPA, so the feed ratio of Tyr is a sum of compositions Tyr and DOPA residues observed for native Pvfp-g or Pvfp-h (Table 1). The polycondensation reaction was also performed with an equi-molar ratio of four NCAs in order to confirm no significant difference in the polycondensation rate among the NCAs (2, 4, 6, 8).

After recovery of the protected copolypeptides (9, 10, 11), viscosity average molecular weight (M_V) was measured for the calculation of the degrees of polymerization (Dps). The observed Dps of the protected copolypeptides were later used for estimation of molecular weight (M_W) of the deprotected copolypeptides (12, 13, 14). Acidolytic removal of the side-chain protecting group, Z, was subsequently conducted in the presence of thioanisole as the scavenger of *in situ* by-product benzyl cations, which often yields undesired adducts on the phenol ring of the Tyr residue. The deprotected copolypeptides were obtained as white powders at yields of 86–90%. The deprotected copolypeptides (12, 13, 14) were soluble in water at 20 w/v%.

In order to determine the actual amino acid compositions after the synthesis, the copolypeptides-g, -h, and -r (12, 13, 14) were hydrolyzed with hydrochloric acid and the hydrolysates were subjected to the amino acid composition analysis (Table 2). The observed composition of the reference copolypeptide-r (14) was Cys:Tyr:Gly:Lys = 23:27:24:26, and this result indicates that the four amino acid NCAs successfully copolymerized into the corresponding polypeptides at approximately equal reaction rate of chain propagation for four different NCAs. This tendency was also observed for the other two copolypeptides-g (12) and -h (13). On the basis of the observed amino acid compositions and the calculated *Dp*s, M_w of the copolypeptides-g, -h, and -r were estimated as $M_w = 7500$ ($Dp = 56$), $M_w = 7450$ ($Dp = 56$), and $M_w = 6940$ (Dp = 51), respectively. Three synthetic copolypeptides have similar average chain lengths and, thus, are appropriate for further characterization.

3.4. Tyrosinase-Mediated Oxidation of Synthetic Copolypeptides

The commercially available preparation of tyrosinase from mushroom usually has two different types of catalytic activities: one is monophenol oxidase activity, where the Tyr residues were oxidized to DOPA, and the other is polyphenol oxidase activity, where the DOPA residues were further converted to DOPA quinone (DQ). In the presence of an appropriate agent such as ascorbic acid (AA), as-produced DQ *in situ* were rapidly reduced to regenerate DOPA [27]. Therefore, the excess amount of AA in the enzyme reaction mixture can apparently suppress production of DQ, inhibiting the oxidative coupling between two DOPA residues. Since the bimolecular adducts of DOPAs and/or DQs cannot be detected in the elution profile of the amino acid analysis, the presence of AA in the enzyme reaction mixture further allows an accurate quantification of DOPA, which is converted from the precursor Tyr residues. The enzyme reaction mixtures of the synthetic copolypeptides, AA, and tyrosinase, were aliquotted at 0, 0.5, 1, 2, 4, 12, and 20 h, and the copolypeptides were immediately hydrolyzed with aqueous methanesulfonic acid, then subjected to the amino acid analysis in order to determine the conversion percentages of DOPA from Tyr (Fig. 3).

The initial molar amount of Tyr was defined as 100%, and the copolypeptide-g was used as the substrate for tyrosinase. As enzymatic oxidation proceeded, the molar percentage of DOPA gradually increased- and, at 20 h, the molar percentage of DOPA reached 24%. As for the reference copolypeptide-r, the conversion percentage from

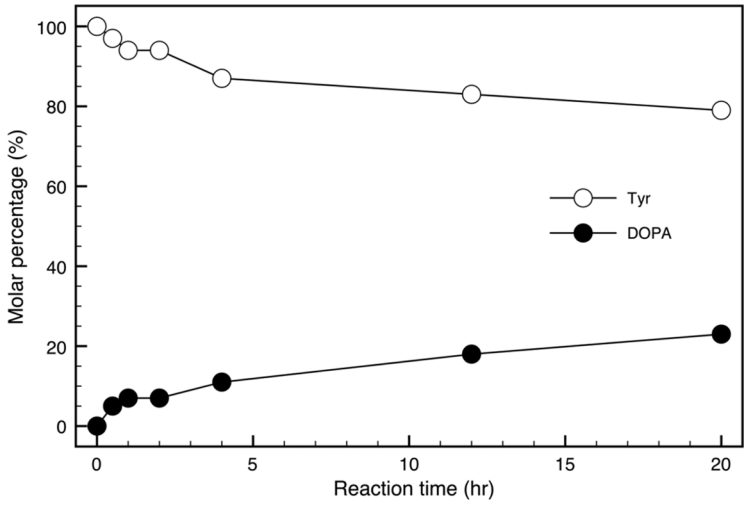

FIGURE 3 Changes in molar percentages of amino acids during enzymatic oxidation of synthetic copolypeptide-g: open circles, Tyr; closed circles; DOPA Enzymatic reaction was carried out in the presence of ascorbic acid as a reducing agent towards DOPA quinone. The enzyme reaction was terminated at predetermined times, and then subjected to hydrolysis, followed by amino acid analysis of the hydrolysate. The initial concentrations of Tyr were defined as 100%.

Tyr to DOPA was 17% and this percentage was rather lower than the copolypeptide-g. The molar percentages of DOPA towards Tyr + DOPA were 64 and 56% for native Pvfp-g and Pvfp-h, respectively (calculated from Table 1). On the other hand, the conversion percentages from Tyr to DOPA were 24% for the copolypeptide-g and 23% (data not shown) for the copolypeptide-h, and these values were much lower than those of native Pvfp-g and Pvfp-h. A highly possible reason for this can be derived from the substrate specificity of tyrosinase. Trypsin digestion of the native Pvfp-g and Pvfp-h liberated several kinds of low molecular weight peptides containing Tyr and DOPA. After the chromatographic separation, followed by the micro-sequencings of the tryptic digests, Gly residues were highly frequently found at the adjacent positions of Tyr/DOPA (data not shown). Since the tyrosinase can efficiently oxidize Tyr residues on the short sequences, likely as –Gly-Tyr–, –Tyr-Gly–, and –Gly-Tyr-Gly–, at the maximum molar percentage of the oxidized product (DOPA) as approximately 80% [28]. In the case of the synthetic copolypeptides-g, -h, and also -r, such kinds of the short sequences preferable for the tyrosinase-mediated oxidation can only be generated by a probability in sequential addition of

the Gly NCA and the Tyr(Z) NCA to the propagating polypeptide chain in the copolymerization process. This probably diminishes the occurrence of the canonical sequence preferred for the tyrosinase-mediated hydroxylation, resulting in less molar percentages of DOPA as compared with native Pvfp-g and Pvfp-h.

3.5. Effect of Enzymatic Cross-Linking on Tensile Shear Strength

The synthetic copolypeptides were subjected to the tensile shear strength measurement in the presence and absence of tyrosinase. In the presence of tyrosinase, the enzyme reaction mixture does not contain AA, so that the DQ produced by the polyphenol oxidaze activity of tyrosinase immediately undergoes quinone-mediated cross-linking. Figure 4 represents the normalized shear strengths towards iron and alumina substrates. The average shear strengths towards the iron substrate in the absence of tyrosinase were 31 kgf/cm^2 for the

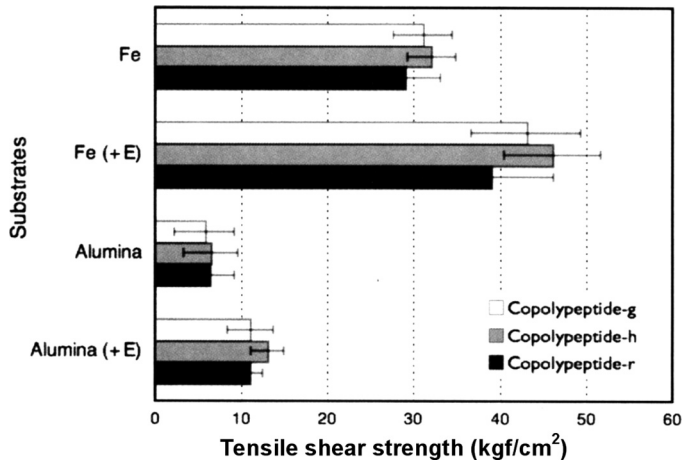

FIGURE 4 Tensile shear strength test using synthetic copolypeptides: open bars, copolypeptide-g; shadowed bars, copolypeptide-h; closed bars, copolypeptide-r. Substrates were iron (Fe) and alumina. Standard deviations among the observed shear force were indicated with error bars. "+E" denotes that the copolypeptide solution was treated with tyrosinase prior to the tensile shear strength test. Unlike in the data in Figure 3, the enzyme reaction was carried out in the absence of ascorbic acid, so that DOPA quinone is generated during enzymatic reaction, inducing quinone-mediated cross-linking between the copolypeptide molecules.

copolypeptide-g, 32 kgf/cm^2 for the copolypeptide-h, and 29 kgf/cm^2 for the copolypeptide-r. In the presence of tyrosinase, the average shear strength clearly increased by the enzymatic cross-linking: copolypeptide-g, 43 kgf/cm^2 (1.3 fold); copolypeptide-h, 46 kgf/cm^2 (1.4 fold); and copolypeptide-r, 39 kgf/cm^2 (1.3 fold). All of the broken faces of the test pieces exhibited cohesive failure, thus indicating that the enzymatic cross-linking of the copolypeptides enhanced the cohesive strength of the polypeptide adhesive.

In the absence of tyrosinase, there is no significant difference in tensile shear strength values toward iron among the three synthetic copolypeptides-g, -h, and -r. On the other hand, the statistical analysis on the tensile shear strength values in the presence of tyrosinase revealed the significant differences in shear strength values between the copolypeptides-g and -r ($P < 0.05$) and between the copolypeptides-h and -r ($P < 0.01$). The differences in shear strength values between the copolypeptides-g and -h was not significant ($P > 0.05$). On the basis of the experimental results on the tyrosinase-mediated oxidation of the copolypeptides-g, -h, and -r, the order in the conversion percentages from Tyr to DOPA were as follows; copolypeptides-g (24%), -h (23%) > -r (17%). Hence, the statistical analysis indicated that the conversion percentage from Tyr to DOPA, followed by the quinone-mediated cross-linking, mostly affects the degree of enhancement of cohesive force in the adhesive layer.

Previously, we reported that the tensile shear strengths of copoly (Tyr^{1}Lys^1) were 35.4 kgf/cm^2 for iron and 9.1 kgf/cm^2 for alumina. After chemical cross-linking of copoly(Tyr^{1}Lys^1) using 2,5-hexanedione, the tensile shear strengths increased to 44.4 kgf/cm^2 for iron and 12.1 kgf/cm^2 for alumina [29]. The fact that degrees of increase in the tensile shear strengths before and after cross-linking were almost the same between the present copolypeptides-g and -h and the previous copoly(Tyr^{1}Lys^1) supported that cross-linking of the adhesive copolypeptides can enhance cohesive force. The tensile shear strengths of the copolypeptides towards alumina also increased in the presence of tyrosinase. The differences in the shear strength values among the copolypeptides were not statistically significant. According to the surface-coupling model, the catecholic side chain of DOPA can more frequently bind to iron than alumina surfaces [30,31], and this is one possible reason for the results on the alumina substrate.

4. CONCLUSION

The present work was conducted to (i) reveal the phenol gland-derived proteins as the adhesive in the biogenesis of *P. viridis* byssus,

(ii) determine characteristic amino acid in the adhesive proteins, and (iii) deduce the roles of the enriched amino acid in the curing of the adhesive plaque. In order to achieve (iii), synthetic copolypeptides were employed as model compounds of the adhesive proteins. In conclusion, (i) Pvfp-h and Pvfp-g are two phenol gland-derived proteins in *P. viridis* byssus, (ii) both Pvfp-g and Pvfp-h are enriched in DOPA and Cys, and (iii) enriched DOPA contributes the protein cross-linking to enhance the cohesive force of the adhesive plaque.

The chemical process of the protein cross-linking in the mussel adhesive proteins was classically understood as a quinone-mediated mechanism. In a marine mussel, *Mytilus californianus*, a Cys-rich component referred to as *M. californianus* foot protein (Mcfp)-6 was recently found. Mcfp-6 is responsible for forming 5-*S*-cysteinyl DOPA to provide a cohesive link between the primer proteins enriched in DOPA and the bulk matrix proteins in the adhesive plaque of *M. californianus* [5,6,32]. According to this new concept, Pvfp-g and Pvfp-h in the *P. viridis* adhesive plaque hypothetically have a dual function as the adhesive primer and the matrix binder. Our research in progress will focus on more detailed characterization of Pvfp-g and Pvfp-h as the plaque-specific adhesive proteins.

ACKNOWLEDGMENTS

This work was partially supported by a Grant-in-Aid for Scientific Research (No. 19390533) and the Global COE Program from the Ministry of Education, Culture, Sports, Science, and Technology of Japan.

REFERENCES

[1] Li, G., Smith, C. S., Brun, Y. V., and Tang, J. X., *J. Bacteriol.* **187**, 257–265 (2005).
[2] Tsang, P. H., Li, G., Brun, Y. V., Freund, L. B., and Tang, J. X., *Pro. Natl. Acad. Sci.* **103**, 5764–5768 (2006).
[3] Zhao, H., Sun, C., Stewart, R. J., and Waite, J. H., *J. Biol. Chem.* **280**, 42938–42944 (2005).
[4] Jensen, R. A. and Morse, D. E., *J. Comp. Physiol. B* **158**, 317–324 (1988).
[5] Zhao, H. and Waite, J. H., *J. Biol. Chem.* **281**, 26150–26158 (2006).
[6] Zhao, H., Robertson, N. B., Jewhurst, S. A., and Waite, J. H., *J. Biol. Chem.* **281**, 11090–11096 (2006).
[7] Waite, J. H. and Tanzer, M. L., *Science* **212**, 1038–1040 (1981).
[8] Kamino, K., in *Biomaterials from Aquatic and Terrestrial Organisms*, Fingerman & Nagabhushanam (Eds.) (Science Publishers, Enfield, 2006), pp. 537–557.
[9] Yamamoto, H., *Bio-Industry* **6**, 684–691 (1989), in Japanese.
[10] Lindner, E., *Biol. Mar, Comun., Congr. Int. Corros. Mar. Incrustaciones,* 5th, pp. 189–212 (1980).

[11] Yonemura, N., Sehnal, F., Mita, K., and Tamura, T., *Biomacromoleeules* **7**, 3370–3378 (2006).
[12] Yamamoto, H., Okada, T., Nagai, A., and Nishida, A., *J. Chem. Soc. Jpn.* **1988**, 1771–1773 (1988), in Japanese.
[13] Kluge, J. A., Rabotyagova, O., Leisk, G. G., and Kaplan, D. L., *Trends Biotechnol.* **26**, 244–251 (2008).
[14] Hawthorn, A. C. and Opell, B. D., *J. Exp Biol.* **206**, 3905–3911 (2003).
[15] Yamamoto, H., *Biotechnology & Genetic Engineering Reviews*, M. P. Tombs (Ed.) (Intercept, Andover, 1996), Vol. 13, Ch. 5, pp. 133–165.
[16] Waite, J. H., Jensen, R. A., and Morse, D. E., *Biochemistry* **31**, 5733–5738 (1992).
[17] Burzio, L. A. and Waite, J. H., *Biochemistry* **39**, 11147–11153 (2000).
[18] McDowell, L. M., Burzio, L. A., Waite, J. H., and Schaefer, J., *J. Biol. Chem.* **274**, 20293–20295 (1999).
[19] Waite, J. H., *Nature Mater.* **7**, 8–9 (2008).
[20] Lucas, J. M., Vaccaro, E., and Waite, J. H., in *Biopolymers*, Steinbuchel (Ed.) (Wiley-VCH, Weinheim, 2003) Vol. 8, Ch. 13, pp. 359–382.
[21] Waite, J. H., *Ann. NY Acad. Sci.* **875**, 301–309 (1999).
[22] Ohkawa, K., Nishida, A., Yamamoto, H., and Waite, J. H., *Biofouling* **20**, 101–115 (2004).
[23] Berger, A., Noguchi, J., and Katchalski, E., *J. Am. Chem. Soc.* **78**, 4483–4488 (1956).
[24] Katchalski, E. and Sela, M., *J. Am. Chem. Soc.* **75**, 5284–5289 (1953).
[25] Vollmer, J. P. and Spach, G., *Biopolymers* **5**, 337–349 (1967).
[26] Hatano, M. and Yoneyama, M., *J. Am. Chem. Soc.* **92**, 1392–1395 (1970).
[27] Rolland, M. and Lissitzky, S., *Biochim. Biophys. Acta* **56**, 83–94 (1962).
[28] Marumo, K. and Waite, J. H., *Biochim. Biophys. Acta* **872**, 98–103 (1986).
[29] Yamamoto, H. and Tanisho, H., *Mater. Sci. Eng.* **C1**, 45–51 (1993).
[30] Sever, M. J. and Wilker, J. J., *Dalton Trans* pp. 813–822 (2006).
[31] Kiss, T., Sovago, I., and Martin, R. B., *J. Am. Chem. Soc.* **111**, 3611–3614 (1989).
[32] Lin, Q., Gourdon, D., Sun, C., Holten-Andersen, N., Anderson, T. H., Waite, J. H., and Israelachvili, J. N., *Pro. Natl. Acad. Sci.* **104**, 3782–3786 (2007).